Environmental Science & Technology

pubs.acs.org/est

Article

Physicochemical Characterization of the Particulate Matter in New Jersey/New York City Area, Resulting from the Canadian Quebec Wildfires in June 2023

Published as part of Environmental Science & Technology virtual special issue "Wildland Fires: Emissions, Chemistry, Contamination, Climate, and Human Health".

José Guillermo Cedeño Laurent,* Hooman Parhizkar, Leonardo Calderon, Denisa Lizonova, Irini Tsiodra, Nikolaos Mihalopoulos, Ilias Kavouras, Mahbub Alam, Mohammed Baalousha, Lila Bazina, Georgios A. Kelesidis, and Philip Demokritou*

Cite This: https://doi.org/10.1021/acs.est.4c02016

Read Online

ACCESS | Metrics & More | Article Recommendations | Supporting Information

ABSTRACT: The global increase in wildfires, primarily driven by climate change, significantly affects air quality and health. Wildfire-emitted particulate matter (WFPM) is linked to adverse health effects, yet the toxicological mechanisms are not fully understood given its physicochemical complexity and the lack of spatiotemporal exposure data. This study focuses on the physicochemical characterization of WFPM from a Canadian wildfire in June 2023, which affected over 100 million people in the US Northeast, particularly around New Jersey/New York. Aerosol systems were deployed to characterize WFPM during the 3 day event, revealing unprecedented mass concentrations mainly in the $WFPM_{0.1}$ and $WFPM_{0.1-2.5}$ size fractions. Peak $WFPM_{2.5}$ concentrations reached 317 $\mu g/m^3$, nearly 10 times the National Ambient Air Quality Standard (NAAQS) 24 h average limit. Chemical analysis showed a high organic-to-total carbon ratio (96%), consistent with brown carbon wildfires nanoparticles. Large concentrations of high-molecular-weight PAHs were found predominantly bound to $WFPM_{0.1}$, with retene, a molecular marker of biomass burning and a known teratogen, being the most abundant (>70%). Computational modeling estimated a total lung deposition of 9.15 mg over 72 h, highlighting the health risks of WFPM, particularly due to its long-distance travel capability and impact on densely populated areas.

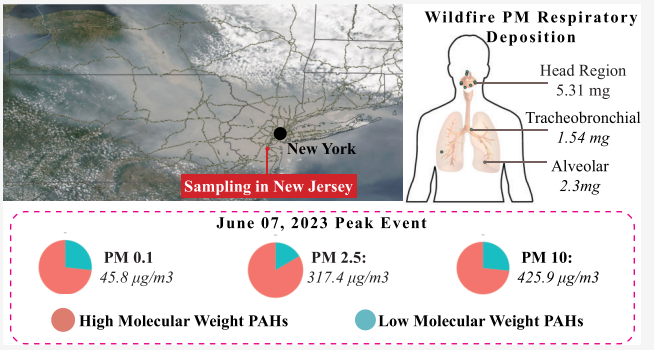

KEYWORDS: *wildfires, wildfire air pollution, ultrafine particles, polycyclic aromatic hydrocarbons, Canadian wildfire, brown carbon*

1. INTRODUCTION

In recent years, the significance of climate-driven wildfires in contributing to air pollution, particularly on particulate matter (PM) levels, has increased at national and global levels.[1] This escalation can be attributed, in part, to climate change, which has intensified the duration, frequency, and magnitude of such events.[2] In addition, a history of fire suppression practices in North America is likely causing wildfires to become larger and more severe.[3]

In the US, over 60,000 wildfires burn an average of 2.8 million hectares of land every year.[4] Due to climate change-driven drought, extreme heat, and reduced snowpack, recent wildfire season lengths are expanding dramatically.[5] In 2020, over 28 million people, approximately 70% of the population in California (CA) experienced more than 100 days of unhealthy air quality as specified by the US Environmental Protection Agency Air Quality Index values above 100 from elevated ambient particulate matter with an aerodynamic diameter of less than 2.5 μm ($PM_{2.5}$) and ozone.[6] During the 2020 wildfires in CA, daily $PM_{2.5}$ levels often reached 350−500 $\mu g/m^3$, significantly higher than the 24 h average limit of 35 $\mu g/m^3$, which is specified by the National Ambient Air Quality Standards (NAAQS).[7]

The impacts of wildfires, however, are not limited to the US. Worldwide, 2.2 billion people were exposed to ≥1 day of substantial wildfire pollution per year in 2010−2019, with the average person having almost 10 days of exposure per year.[8] The

Received: February 27, 2024
Revised: June 28, 2024
Accepted: July 1, 2024

same analysis determined that, globally from 2000 to 2019, the population weighted average $WFPM_{2.5}$ exposure was 2.5 $\mu g/m^3$. It is significant to mention that, since WFPM is dominated by nanoscale PM, which has less mass compared to micron-scale particulates, a 2.5 $\mu g/m^3$ add on is translated to millions of particles per volume of air with different and unique chemical composition. Therefore, relying on PM mass concentrations may underestimate the associations between WFPM and health outcomes given the nanoscale nature of such particles. Furthermore, wildfire air pollution poses a significant health threat, particularly to socially vulnerable Americans living in environmental justice communities already burdened with compromised air quality. Davies et al., 2018, identified 29 million Americans at risk for extreme wildfires, of which 12 million belonging to Black, Hispanic, or Native American communities face approximately 50% greater vulnerability to wildfires compared to other census tracts.[9] This vulnerability to wildfires compounds the frail situation of minority groups, which are disproportionately affected by other environmental risks.[10] In toto, in the United States and globally, the impact of wildfires on air quality has been profound, to the extent of reversing or stagnating the progress made in air quality improvements over the past two decades.[11]

Wildfire smoke is a complex mixture of particles and gaseous pollutants, with particles in the fine (less than 2.5 μm, $PM_{2.5}$) and contain ultrafine or nano (<100 nm, $PM_{0.1}$) range.[12−14] $PM_{2.5}$ particles, and especially its $PM_{0.1}$ size fraction, are of great health concern as they can penetrate and deposit to the deepest part of the lungs, cross the alveolar epithelium and other biological barriers, enter blood circulation, and accumulate in peripheral organs beyond the lungs.[15] In addition to health effects, WFPM absorbs[16] and scatters[17] the solar radiation differently compared to PM emitted from other sources and thus can alter radiative forcing and affect climate change as well. So, a detailed physicochemical characterization of spatiotemporal properties of WFPM is essential to quantify accurately its impact on public health and climate.

The few exposure assessment studies that have characterized WFPM chemical composition in areas with wildfires demonstrate that it contains primarily organic carbon (OC, >97%) and less elemental carbon (EC).[13,18−20] Its complex chemical composition is also unique and includes heavy metals, polycyclic aromatic hydrocarbons (PAHs), plasticizers, flame retardants, and industrial solvents[12,13,21] due to combustion of both biomass and man-made structures.[22] The authors showed in their recently published by Singh et al. study[20] that the "fuel" and combustion characteristics affect its chemical composition.

The unique physicochemical characteristics of the WFPM may result in higher toxicity than urban background PM, which is mostly generated from fossil fuel combustion.[23] For example, *in vitro* and *in vivo* toxicological studies show that WFPM exposure causes higher levels of oxidative stress and lung inflammation due to the presence of more polar organic compounds with higher oxidative potential compared to ambient $PM_{2.5}$.[13,20]

The impact of WFPM on human disease remains largely unquantified, demanding more epidemiological studies[24] and improved exposure assessment methods that takes proper consideration of its unique physicochemical and toxicological profile. Emerging epidemiological studies from around the world have found that, at similar ambient exposure levels, WFPM is associated with a higher risk of respiratory,[23,25,26] cardiovascular,[27] and neurological health outcomes[28] and a higher risk of all-cause mortality[26,29] than non-WFPM, which can be attributed to differences in their chemical composition.

While some knowledge gaps have been addressed in response to extensive wildfires predominantly in the U.S. West Coast, the 2023 Canadian Wildfire season highlighted their potential to significantly affect other regions and major metropolitan areas, including the U.S. Northeast and Midwest. The 2023 wildfire season in Canada sets new records, with over 6132 fires burning more than 16.5 million hectares by September 5, double the 1989 record of burnt area by wildfires in Canada.[30] Canada experienced its warmest May−July period in over 80 years, breaking previous national temperature records for the two-month period by 0.8 °C. From June 1 to 25, more land burned in southern Quebec than in the previous 20 years combined, leading to the largest single fire ever recorded in southern Quebec, consuming 460,000 ha.

In June 2023, wildfire smoke from Quebec, Canada, rose into the jet stream and was transported into New York City (NYC), New Jersey (NJ), and other major metropolitan areas in the Northeast, resulting in multiple days of catastrophic air quality with $PM_{2.5}$ levels reaching over 300 $\mu g/m^3$[31] and affecting over 100 million Americans. On June 7, the 11 Department of environmental Pollution (DEP) monitoring sites in New York City recorded the worst air quality level in over 50 years. The observed maximum daily mean $PM_{2.5}$ concentration reached 148.3 $\mu g/m^3$, nearly 10 times the 24 h air quality guideline issued by the World Health Organization (WHO).

In this study, a detailed physicochemical characterization of the WFPM using real-time and time-integrated aerosol instrumentation and analytical methods was performed in Piscataway, NJ, approximately 43 miles southwest from New York City during the days of the most severe impact from this Canadian wildfire incident (June 6−9, 2023). This paper aims to elucidate the complex physicochemical properties of PM in this unique context, contributing to a deeper understanding of the environmental and health impacts of wildfire-induced air pollution episodes in a major metropolitan and heavily populated area.

2. METHODS

2.1. Sampling Site Description. The PM monitoring site was located at the Rutgers University Piscataway Campus, approximately 43 miles southwest from New York City. A schematic of the sampling equipment is shown in Supplemental Figure S1. Real-time PM monitoring and time-integrated PM sampling equipment were located in the courtyard adjacent to the Environmental and Occupational Health Sciences Institute (EOHSI) at a sampling height 1.5 m above ground level. Four sampling phases throughout the 72 h wildfire incident totaling 60 h were conducted between June 6 and June 9, 2023 as follows: (1) start phase (Phase A): June 6 19:50−June 7 14:00; (2) peak phase (Phase B): June 7 15:00−June 7 19:06; (3) postpeak phase (Phase C): June 7 20:12−June 8 12:02; (4) end phase (Phase D): June 8 15:22−June 9 13:28.

In addition, 1 h average mass concentrations of $PM_{2.5}$, nitrogen oxides (NO_x), and ozone (O_3) were obtained from the US EPA Photochemical Assessment Monitoring Station (AQS Site Code 340230011) 7.3 miles from the monitoring site. Carbon monoxide 1 h average concentrations were also obtained from the Newark Firehouse monitoring station (AQS Site Code 340130002), 22.3 miles northeast of our monitoring site. Data included in this analysis were subject to quality data assurance by US EPA.

https://doi.org/10.1021/acs.est.4c02016
Environ. Sci. Technol. XXXX, XXX, XXX−XXX

2.2. Wildfire Smoke Transport Modeling. Backward air mass trajectories during the wildfire incident were examined using the U.S. National Oceanic and Atmospheric Administration, Air Resources Laboratory (NOAA-ARL) Hybrid Single-Particle Lagrangian Integrated Trajectory (HYSPLIT) transport, and the dispersion model. The calculated trajectories traced back up to 36 h from the Rutgers monitoring site using 500 and 1000 m as starting atmospheric heights above ground level. These heights were chosen to avoid inaccuracies from turbulence and frictional effects at lower heights.[32]

2.3. Time-Integrated and Size-Fractionated WFPM Sampling. Size-fractionated WFPM ($WFPM_{0.1}$-PM below 0.1 μm, $WFPM_{0.1-2.5}$-PM between 0.1 and 2.5 μm, $WFPM_{2.5-10}$-PM between 2.5 and 10 μm, and $WFPM_{>10}$=PM above 10 μm aerodynamic diameter) was collected using Harvard Compact Cascade Impactors (CCIs)[33] and used for deriving mass particle concentrations and for offline chemical characterization. $PM_{0.1}$ was collected on prebaked quartz fiber filters (Pallflex Tissuquartz filter: 47 mm diameter, Pall Corporation, Port Washington, NY) for Elemental Carbon and Organic carbon (EC-OC) analysis, as well as with Teflon filters (PTFE membrane disc filter: 2 μm pore size, 47 mm diameter, Pall Corporation, Port Washington, NY) for inductively coupled plasma mass spectrometry (ICP-MS) analysis. Larger PM fractions were collected on polyurethane foam (PUF) substrates, as described previously.[33,34] Further details are included in the Supporting Information section. Given the large amount of $WFPM_{0.1}$ and $WFPM_{2.5}$ collected during the peak phase (Phase B), these samples were chosen for the EC-OC, PAH, and elemental analysis described in the following sections.

2.4. Real-Time WFPM Monitoring. A Scanning Mobility Particle Sizer (SMPS model 3080, TSI Inc., Shoreview, MN) was used to measure in real-time particle number concentrations in the 5−300 nm mobility diameter range. For larger particles (0.5−20 μm aerodynamic diameter), an Aerodynamic Particle Sizer (APS, model 3321, TSI Inc., Shoreview, MN) was used.

2.5. WFPM-Bound Polyaromatic Hydrocarbons (PAHs) Analysis from the Peak Phase. For PAH analysis of WFPM size fractions collected from the peak phase, the protocol described in Tsiodra et al.[35] was used with slight modifications (see the Supporting Information). The analysis focused on the identification of 25 PAHs with molecular weight between 178 and 278 g/mol. The parent PAHs species are phenanthrene (Phe), anthracene (Ant), fluoranthene (Fla), pyrene (Pyr), benzo[a]anthracene (B[a]A), chrysene (Chr), benzo[b,j,k]-fluoranthenes (B[bjk]F), benzo[e]pyrene (B[e]P), benzo[a]-pyrene (B[a]P), indeno (1,2,3-c,d) pyrene (IndP), dibenzo-[a,h]anthracene (dBaAnt), and benzo[g,h,i]perylene (B[ghi]-Per), and the methylated species are 1-methylphenanthrene (1-C1-Phe), 2-methylphenanthrene (2-C1-Phe), 3-methylphenanthrene (3-C1-Phe), 9/4 methylphenanthrene (9/4 C1-Phe), 2,6-dimethylphenanthrene (2.6-DMP), 2,7-dimethylphenanthrene (2.7-DMP), 3,6-dimethylphenanthrene (3.6-DMP), 1.3/2.10/3.9/3.10-dimethylphenanthrene (1.3/2.10/3.9/3.10-DMP), 1.6/2.9-dimethylphenanthrene (1.6/2.9-DMP), 1.7-DMP-Pimanthrene (1.7-DMP), methyl-fluoranthene/pyrene (C1-202), retene (Ret), and methyl chrysenes (MChry).

2.6. WFPM Organic and Elemental Carbon Analysis from the Peak Phase. The analysis of organic and elemental carbon (EC-OC) was performed on the $PM_{0.1}$ quartz filter from the peak phase, creating dedicated 1 cm^2 punches, using the thermal-optical transmission (TOT) technique with a Sunset carbon analyzer (Sunset Laboratory Inc., Portland, OR, USA) and the EUSAAR2 thermal protocol described in detail by Cavalli et al.[36] Given that EC-OC analysis is a thermally destructive method, and considering that the larger PM size fractions were collected on PUF substrates, it was not possible to analyze the remaining size fractions for EC-OC.

2.7. $WFPM_{0.1}$ Inorganic Elemental Analysis. The elemental particle composition at the individual particle level was determined by SP-ICP-TOF-MS (TOFWERK, Thun, Switzerland) as described in detail in our previous studies[37] and in the Supporting Information section. Select elemental ratio distributions were determined on a particle-by-particle basis taking into account all particles.

2.8. WFPM Respiratory Deposition Modeling. Multiple-Path Particle Dosimetry Modeling (MPPD V3.01) was used to estimate the total particle deposition in the human lung airway from the head to the alveolar region.[38] The calculations were done using the Yeh/Schum symmetric human model[39] with a functional residual capacity of 3300 mL and a head volume of 50 mL. The model assumes that human bodies are exposed at an upright orientation to a mono disperse aerosol concentration with PM size-specific mass median aerodynamic diameter derived gravimetrically in the peak phase as described above and effective density summarized in Table S3. The nasal breathing frequency was set to 12 breaths/min, the tidal volume to 625 mL, and the inspiratory fraction to 0.5.[40] The deposited mass was calculated for the 72 h exposure period of the event.

3. RESULTS AND DISCUSSION

3.1. Wildfire Plume Transport Analysis Using HYSPLIT Backward Trajectories. Wildfire plume transport analysis from HYSPLIT backward trajectories confirms that air masses during the incident originated in the Quebec active wildfire were transported southward to the monitoring site. In more detail, Figure 1 shows the air mass taking between 18 and 24 h to arrive at the Rutgers Piscataway site on June 7 at 18:00 EDT, around the peak of the wildfire incident. Prior to June 5, trajectories show air originating close to the Canadian province of New Brunswick, where active medium-sized wildfires were taking place on June 2. Trajectories progressively shifted west, and on June 6, air masses were coming southward directly from the Quebec province (Figure S4).

Documented evidence of Quebec wildfire impacts in the US Northeast region dates to a wildfire incident in July 2002. In that incident, backward trajectory analysis suggested longer transport times from the active wildfire to Pittsburgh, PA and Baltimore, MD in approximately 36−48 h.[41,42]

3.2. $PM_{2.5}$ Mass Concentrations and Gaseous Pollutants from the EPA Monitoring Site. Figure 2a shows the time evolution of ambient $PM_{2.5}$ mass concentrations from the US EPA Photochemical Assessment Monitoring Station throughout the wildfire incident. $PM_{2.5}$ started increasing on June 6, reaching a 24 h mass concentration of 32.7 $\mu g/m^3$. On June 7, the $PM_{2.5}$ 24 h average increased to 181.4 $\mu g/m^3$, peaking at 1800 EDT with a maximum 1 h average concentration of 334.6 $\mu g/m^3$. The two subsequent days June 8 and 9 still experienced higher than usual $PM_{2.5}$ concentrations, with 24 h averages of 146.7 and 22 $\mu g/m^3$, respectively.

The 24 h average $PM_{2.5}$ mass concentrations experienced on June 7 in this area (181.4 $\mu g/m^3$) were the highest on more than 50 years of ambient air quality records and were 5.2 times higher than the 24 h average limit set by the National Ambient Air Quality Standards (NAAQS). In comparison to the July 2002 wildfire incident, air quality measurements back then in

https://doi.org/10.1021/acs.est.4c02016
Environ. Sci. Technol. XXXX, XXX, XXX−XXX

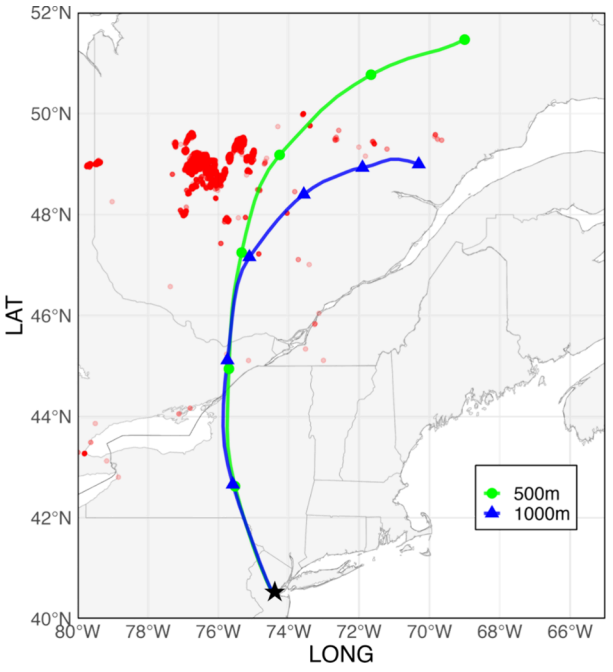

Figure 1. HYSPLIT backward trajectories calculated at 500 and 1000 m above ground level for air mass arriving at the Rutgers Piscataway Campus (Lat: 40.5240, Long: −74.4684; depicted on the figure with a star) on June 7th, 2023 1800 EDT. Red dots represent active forest fire sites on June 7th according to the Canadian Wildland Fire Information system (https://cwfis.cfs.nrcan.gc.ca/home; consulted 12/01/2023).

Baltimore, Pittsburgh, New York, and Boston showed 24 h average $PM_{2.5}$ concentrations between 63 and 86 $\mu g/m^3$,[41,43] which are $PM_{2.5}$ mass concentrations considerably lower than those reported in this study.

Figure 2b depicts the progressive increase in local outdoor levels of CO starting on June 5, peaking on June 7 at between 1700 and 1900 EDT, and going back to preincident levels on June 11. A maximum 1 h average for CO of 1.5 ppm was registered on June 7 at 1800 EDT.

During the incident, NO_x and ground-level O_3 levels showed a typical diurnal pattern, with two pronounced O_3 surges on June 2 and June 6 when 1 h average O_3 reached the maximum concentrations of 111 and 65 ppb, respectively (Figure 2b). O_3 concentrations on June 7 (peak phase) were noticeable lower than the previous day despite the dramatic increase in $PM_{2.5}$ and CO concentrations. The small O_3 concentrations on June 7 could be attributed to high $PM_{2.5}$ concentrations that contain mostly OC. Such "brown nanoparticles" scatter strongly solar light[44] and may reduce the transmission of solar irradiation resulting in reduction of O_3 production. Photoacoustic extinctiometer measurements of the WFPM strong light scattering and absorption on June 7 support this claim and will be presented in the aforementioned companion paper focusing on WFPM optical properties.

3.3. Time-Integrated WFPM Mass Size Distributions. The time evolution during the event of WFPM mass concentration for each size fraction is shown in Figure 3. $WFPM_{0.1}$ and $WFPM_{0.1-2.5}$ mass concentrations experienced a sharp increase starting in the late afternoon of June 6 during the start phase ($WFPM_{0.1}$ = 48.1 $\mu g/m^3$ and $WFPM_{0.1-2.5}$ = 48.1 $\mu g/m^3$), reaching the maximum around June 7 afternoon (peak phase, $WFPM_{0.1}$ = 145.8 $\mu g/m^3$ and $WFPM_{0.1-2.5}$ = 171.6 $\mu g/m^3$). Concentrations reduced gradually on June 8 (postpeak phase, $WFPM_{0.1}$ = 68.3 $\mu g/m^3$ and $WFPM_{0.1-2.5}$ = 83.7 $\mu g/m^3$) and June 9 (end phase, $WFPM_{0.1}$ = 21.9 $\mu g/m^3$ and $WFPM_{0.1-2.5}$ = 17.0 $\mu g/m^3$).

As shown in Figure 3, $WFPM_{0.1}$ mass concentration during the peak phase is at the same level with $WFPM_{0.1-2.5}$. This is expected, primarily because, as shown both in this study (Figure 4), and as published by our group before,[19,20] WFPM are by number mostly nanoscale size particles. It is important to mention that the $WFPM_{0.1-2.5}$ size fraction contains the "tail" of the wildfire-emitted particles but also particles from other local and other sources inclusive of traffic.[45] Also important is that both the time course and WFPM mass concentrations agreed with the data from the EPA monitoring station at Rutgers shown in Figure 2a. Other studies reporting PM size distribution from large-scale mass burning incidents have found large increases predominantly in $PM_{0.1}$[46] and $PM_{1.0}$.[12] Further details on the size distributions are reported in the Supporting Information section.

3.4. $WFPM_{0.1}$ EC-OC. Analysis of carbon mass fractions during the peak phase was dominated by OC (139.7 $\mu g/m^3$) in comparison to EC (6.1 $\mu g/m^3$) resulting in an organic-to-total carbon ratio, OC/TC = 96%. This is consistent with the high OC/TC associated with biomass burning.[19,20] The literature reports a wide range of OC/TC values attributed to differences in the fuel type, burning process (i.e., flaming vs smoldering),[47] degree of photochemical aging,[48] and contribution of wildfire smoke with respect to local pollution sources.[13] Importantly, a source apportionment modeling to attribute the contributions to PM pollution of other sources would be important to pursue in a future study.

The EC/TC fraction of 4.3% observed here is within the range of reported values (EC/TC= 1−5.5%) in the literature for prescribed fires and wildfires.[49] During the Quebec wildfires of 2002, a maximum EC/TC = 2.7% was measured in Baltimore, MD.[42] The higher OC relative content in such measurements could have resulted from plume aging during the longer transport times in that episode (36−48 h). Moreover, based on light absorption and scattering measurements collected by the authors and presented in an accompanying manuscript, the WFPM sampled on June 7 is less photochemically aged compared to that sampled on June 8.

3.5. WFPM PAH Analysis. Concentrations of the 20 detected out of 25 targeted PAHs in PM size-speciated samples from the peak phase are shown in Figure 4. Total PAH concentration was 98.1 ng/m^3 of which 13.8 ng/m^3 (14.1%) was found in $PM_{0.1}$, 40.5 ng/m^3 (41.3%) in $PM_{0.1-2.5}$, 30.6 ng/m^3 (31.1%) in $PM_{2.5-10}$, and 13.2 ng/m^3 (13.4%) in $PM_{>10}$. High-molecular-weight (HMW, >220g/mol) PAHs, associated with higher bioaccumulation and toxicity, and characteristic of biomass burning, were found at higher concentration (66.3 ng/m^3, 67.6%) than low-molecular PAHs (LMW, <220 g/mol). LMW were mostly found on PM size fractions larger than $PM_{2.5}$, and virtually none were detected in the nanoparticle range (0.08%).

Only 8 of the detected PAHs are part of the 16 PAHs in EPA's priority list, accounting for 26.3% of the PAH total concentration (Figure S2). In terms of individual PAHs, retene had the highest overall concentration with 37.4 ng/m^3 in $PM_{2.5}$ and 53.7 ng/m^3 in PM_{10}, followed by phenanthrene ($PM_{2.5}$ = 4.2 ng/m^3 and PM_{10} = 11.0 ng/m^3) and methylphenanthrene isomers 1-C1-Phe ($PM_{2.5}$ = 1.3 ng/m^3 and PM_{10} = 3.2 ng/m^3) and 2-C1-Phe ($PM_{2.5}$ = 0.7 ng/m^3 and PM_{10} = 3.0 ng/m^3).

https://doi.org/10.1021/acs.est.4c02016
Environ. Sci. Technol. XXXX, XXX, XXX−XXX

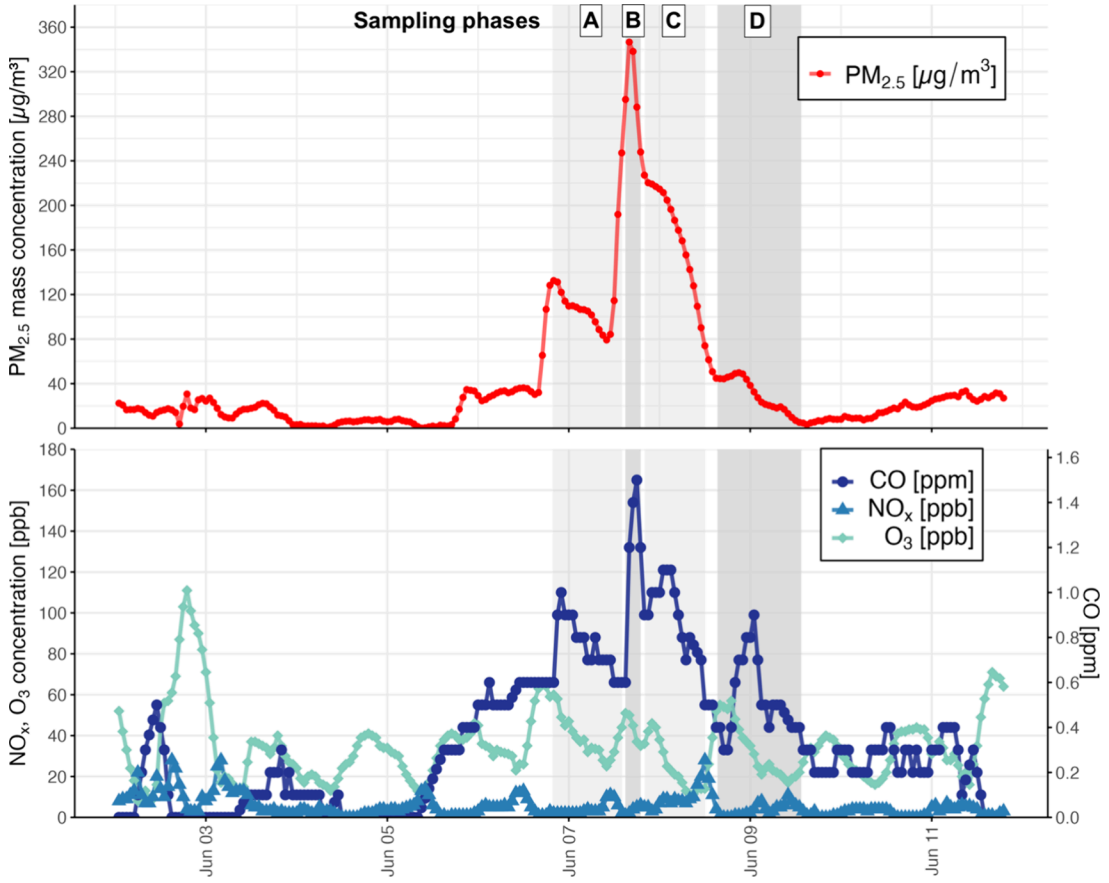

Figure 2. One hour average ambient concentrations for (a) $PM_{2.5}$; and (b) CO, O_3, and NO_x. $PM_{2.5}$ and O_3 data were obtained from the US EPA Photochemical Assessment Monitoring Station near Rutgers University and CO and NO_x from the EPA Newark site. Shaded gray areas indicate the sampling phases with real-time and integrated measurements at Rutgers Piscataway Campus.

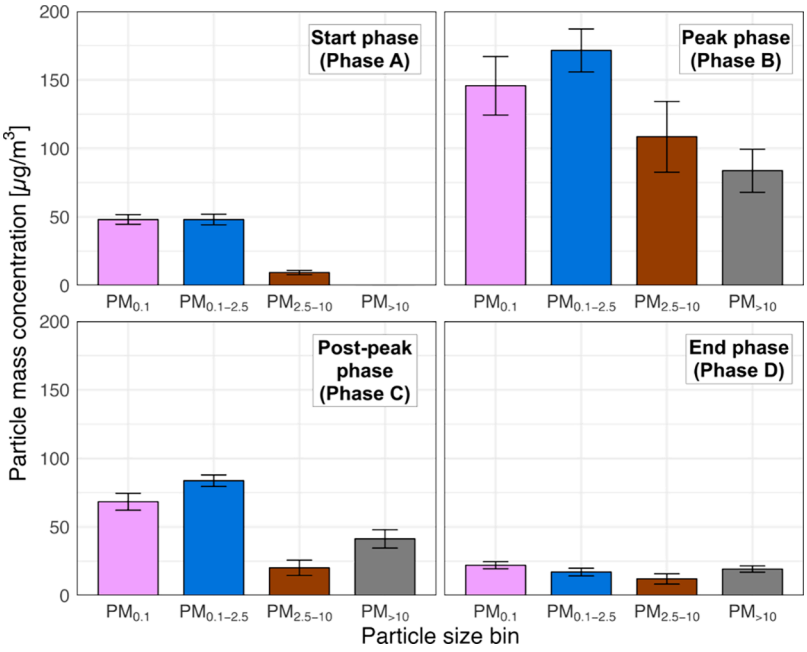

Figure 3. Time-integrated ambient particle mass concentration as a function of PM aerodynamic size fraction from four sampling phases: start phase (Phase A): June 6 19:50–June 7 14:00; peak phase (Phase B): June 7 15:00–June 7 19:06; postpeak phase (Phase C): June 7 20:12–June 8 12:02; end phase (Phase D): June 8 15:22–June 9 13:28. Error bars show 95% confidence interval.

These four isomers represented 80.2 and 83.8% of the total PAH concentration in $PM_{2.5}$ and PM_{10}, respectively.

Elevated concentrations of PAH congeners such as retene (Ret), phenanthrene (Phe), and fluoranthene (Fla) were found

https://doi.org/10.1021/acs.est.4c02016
Environ. Sci. Technol. XXXX, XXX, XXX−XXX

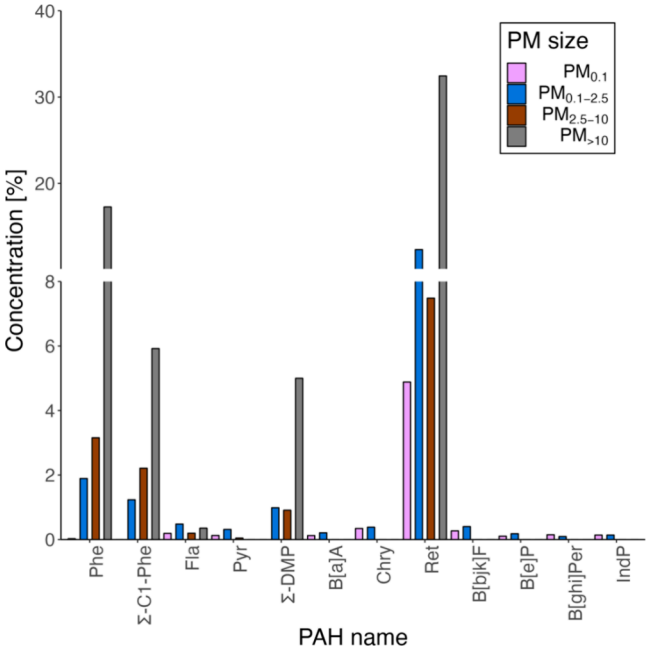

Figure 4. Percent mass concentration of size-fractionated PM-bound PAHs collected in the peak phase (Phase B). Detected methylated phenanthrenes are shown aggregated in Σ-C1-Phe and Σ-DMP.

in the peak period samples, suggesting a PAH emission profile similar to previous reports from boreal forests wildfires in North.[50] Portugal fires in 2009 were also dominated by Ret and Phe concentrations.[51] The predominance of wildfire pollution in this analysis is validated by PAH diagnostic ratios above 0.5 for Fla/Pyr and IndP/B[ghi]Per, both associated with biomass combustion.[52] Furthermore, the diagnostic ratio of Ret/(Ret+Chry) is very high (>0.9) for $WFPM_{0.1}$ and $WFPM_{0.1-2.5}$ confirming the hypothesis that the collected WFPM is dominated by softwood combustion.[53]

Two important findings in this study are (1) the high PAH concentrations during the peak phase and (2) the large presence of HMW PAHs, predominantly in the nanoparticle range. While comparisons with previously reported wildfires are difficult due to the variety of factors involved including pollution intensity, fuel type, atmospheric transport conditions, among others, the PAH concentrations in our samples were higher than previously reported for wildfire incidents with similar WFPM concentrations. Reported for strong haze episodes in southern Thailand show total PAH and total suspended PM concentrations of 2.5 ng/m^3 and 40 μg/m^3, respectively, in 2019, and 34.1 ng/m^3 and 340.1 μg/m^3, respectively, in 2015.[46] These concentrations are lower than the total PAH concentration of 98.1 ng/m^3 in PM_{TSP} during the peak phase (PM_{TSP} = 509.6 μg/m^3). Higher concentrations of HMW PAHs in fine and ultrafine PM size fractions agree with previous reports.[12,46,54]

Retene concentrations per mass WFPM during the peak phase (226.8 μg/g) are 2 orders of magnitude higher than those reported by Verma et al. (6.68 μg/g).[13] This discrepancy exists despite both studies reporting similar 24 h mean $PM_{2.5}$ concentrations (Verma et al.: 140−150 μg/m^3; this study: 148 μg/m^3 on June 7th). One potential explanation is that, in the Verma et al., 2009, the distance from the wildfire to the monitoring site is considerably shorter than in our study, with potential shorter aging times. In their study, they report a higher B[a]P/(B[a]P+B[e]P) ratio, which is used for the characterization of aerosol aging.[55] The complete absence of B[a]P in our study suggests a higher degree of aging, since B[a]P is more reactive than B[e]P.[56] It is worth noting that, while in this study, background levels of retene were not measured, such levels are expected to be miniscule, given the absence of any local wildfires of coniferous forests during the Canadian wildfire event or other significant biomass burning (e.g., for heating purposes).

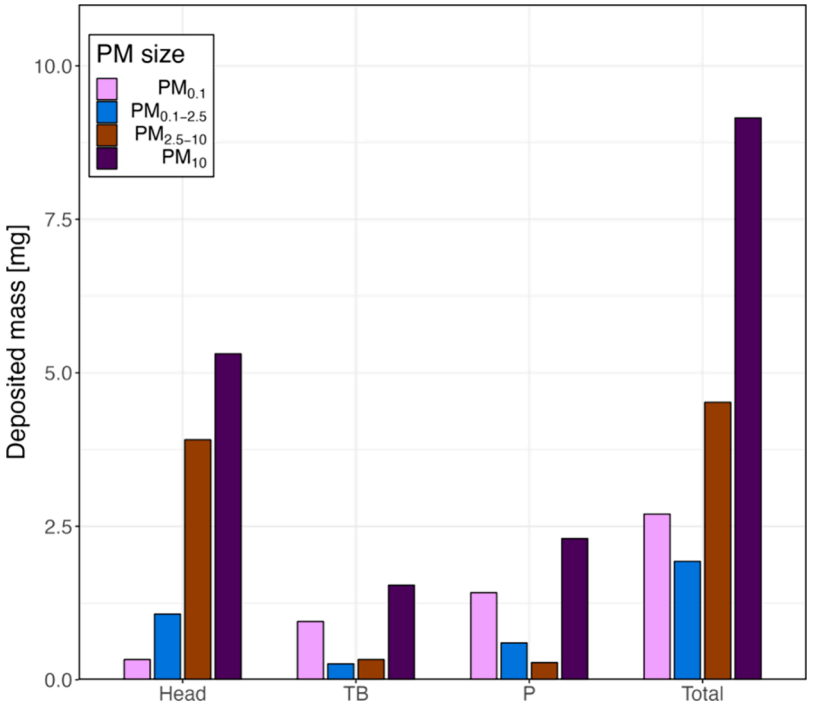

Figure 5. Size-fractionated mass of deposited wildfire PM in the head, tracheobronchial (TB), pulmonary (P), and total region of the human respiratory tract derived by MPPD for a 72 h exposure to concentrations measured during the peak phase (Phase B).

https://doi.org/10.1021/acs.est.4c02016
Environ. Sci. Technol. XXXX, XXX, XXX−XXX

3.6. $WFPM_{0.1}$ Inorganic Elemental Analysis. Single particle analysis detected 12 inorganic elements in the $PM_{0.1}$ particle size fraction, including a combination of crustal elements (Fe, Mn, and Al) and metals associated with anthropogenic sources (e.g., Ba, Ti, Cr, Zn, Pb, Sn, Ni, Sb, and Cu; Figure S3). Iron, Ba, and Zn were dominated by single-metal nanoparticles (NPs). In contrast, all other elements were dominated by multimetal NPs. Most of the multimetal NPs were Fe-bound. The elemental ratios of Ti/Fe, Mn/Fe, Cr/Fe, Al/Fe, Ba/Fe, and Ni/Fe are higher than the average crustal ratios and are typical of those observed in vegetation and atmospheric deposition wildfire ash (e.g., Ti/Fe = 0.001−2.0, Mn/Fe = 0.01−5.0, Cr/Fe = 0.002−0.5, Al/Fe = 0.05−20, Ba/Fe = 0.005−0.2, and Ni/Fe = 0.01−0.2), with higher elemental ratios in the atmospheric deposition ash relative to the vegetation ash[57] suggesting that these NPs originated from the Canada fire plume.

While the concentration of transition elements such as Mn, Cr, and Cu in the reported WFPM samples (Figure S3) was low, their presence is relevant for environmental and human health implications. Cu and Mn nanoparticles have been found to induce oxidative stress, form reactive oxygen species, and lead to DNA damage among other effects.[58] Wildfire-specific characteristics such as fuel type, location, and fire temperature influence these metals' availability and toxicological properties in WFPM,[59] but potential synergistic effects from other chemical compounds remain poorly understood, and mechanistic toxicological studies are needed.

3.7. WFPM Respiratory Deposition Modeling. Particle mass deposition in the human lung airway during the 72 h event from the MPPD modeling is shown in Figure 5. Mass deposition for $WFPM_{0.1}$ and $WFPM_{0.1-2.5}$ size fractions was the highest in the pulmonary region, followed by the head and tracheobronchial regions. Notably, the deposition of particles in the respiratory tract is size specific.[60] In other words, the three inhalable size fractions, namely, $WFPM_{0.1}$, $WFPM_{0.1-2.5}$, and $WFPM_{2.5-10}$, will deposit differentially in various areas of the respiratory tract. The WFPM10 is the sum of all three size fractions and their deposition in each respiratory tract area.

Total deposition was 9.15 mg for the inhalable $WFPM_{10}$, predominantly in the head region (5.31 mg). The deposited mass rate per minute for each individual region of the respiratory tract and per respiratory surface area are summarized in Table S3. Based on this, the estimated PM_{10}-bound PAH mass deposition values in the head, tracheobronchial, and pulmonary were 2.9, 0.8, and 1.3 mg, respectively, during the 72 h wildfire incident. Given the known effects of PAHs on disease development including carcinogenicity and metabolic diseases among others,[61] more toxicological studies are needed to assess potential health effects.

The large PM doses across the human respiratory system as a result from this 72 h incident and their unique and complex chemical load (e.g., PAHs, heavy metals) raise concerns for potential adverse health effects and disease development, especially among susceptible and vulnerable populations. Emerging epidemiological studies associated with this particular wildfire event have reported that asthma-associated emergency department (ED) visits in New York State on June 7 rose 81.9% with respect to before the wildfire incident (June 1−June 5 2023).[62] In another study in New York City, a 10 $\mu g/m^3$ increase in $PM_{2.5}$ was associated with an asthma ED incidence rate ratio (IRR) of 1.03 (95% CI, 1.02−1.04).[63]

Health impacts of WFPM are expected from the detrimental effects on other organs beyond the respiratory system. Given the large proportion of deposition in the head region and the known translocation to the brain via the olfactory nerve of nanoscale particles,[64] it is important to consider the potential effects of wildfire pollution on the nervous system. Several epidemiological studies have linked WFPM with impacts on cerebrovascular ED visits,[65] mental health,[66] cognitive function (Cleland et al. 2023), and performance on standardized tests.[67]

Similarly, emerging findings from other incidents shown associations of $WFPM_{2.5}$ with reproductive health outcomes such as increased risk of preterm birth[68] and birth defects.[69] Of a particular interest is the presence of high molecular PAHs, which have linked to long-term carcinogenesis and have also been associated with a very high odds ratio (OR = 2.74, 95% CI, 2.24−3.34) of preterm birth.[70] More epidemiological and toxicological studies are needed to assess the impact on health from this and other wildfire events.

Our study confirms the complex chemistry of WFPM, characterized by its elevated content of toxicologically concerning species such as high molecular PAH, found predominantly in the nanoparticle scale. Retene, a molecular marker of conifer biomass pyrolysis,[71] represented more than 70% mass concentration of all detected PAHs. Evidence from *in vitro* studies links retene to induction of oxidative stress in the lung,[72,73] hepatotoxicity,[74] neurotoxicity,[75] developmental toxicity, and endocrine disruption.[76] Unfortunately, there are extensive knowledge gaps on the effects of WFPM-bound PAHs from ambient air exposures. As explained elsewhere,[73,77] part of this knowledge gap is due to the exclusion of PAHs associated with biomass burning, such as retene, from the EPA priority list.

While epidemiological studies have found significant associations between WFPM exposure and respiratory, cardiovascular, neurological, and reproductive health outcomes, the mechanisms behind them are largely unknown. More toxicological studies are needed to understand potential adverse outcome pathways related to WFPM. This is especially important since projections based on current climate change trajectories indicate an increased frequency and intensity of regional wildfires, suggesting a heightened risk of similar wildfire events in the future and highlighting the importance of understanding the health implications of such events.[78]

As wildfires increasingly contribute to air pollution and air quality, affecting the health and well-being of millions, it is imperative that these events no longer be considered exemptions under EPA regulatory standards. Historically, such natural events were seen as rare and unpredictable, leading to their exemption from daily and annual air quality evaluations. However, with climate change enhancing the frequency and intensity of wildfires, these are no longer sporadic events but recurrent ones, necessitating a shift in regulatory paradigms. In summary, the magnitude, size distribution, and chemical composition of WFPM in a major densely populated metropolitan area warrant further studies to better understand the impact on human health.

■ ASSOCIATED CONTENT

Supporting Information

The Supporting Information is available free of charge at https://pubs.acs.org/doi/10.1021/acs.est.4c02016.

TOF MS analytical details, MPPD deposition rate per region, sampling equipment schematic, PAH mass

https://doi.org/10.1021/acs.est.4c02016
Environ. Sci. Technol. XXXX, XXX, XXX−XXX

concentration per PM size fraction, NP elemental analysis, elemental ratios distributions in NPs, and offline characterization methods in detail (PDF)

AUTHOR INFORMATION

Corresponding Authors

José Guillermo Cedeño Laurent − *Department of Environmental and Occupational Health and Justice, School of Public Health, Rutgers University, Piscataway, New Jersey 08854, United States; Nanoscience and Advanced Materials Center, Environmental and Occupational Health Sciences Institute, Rutgers University, Piscataway, New Jersey 08854, United States;* orcid.org/0000-0001-7098-0954; Email: memo.cedeno@rutgers.edu

Philip Demokritou − *Department of Environmental and Occupational Health and Justice, School of Public Health, Rutgers University, Piscataway, New Jersey 08854, United States; Nanoscience and Advanced Materials Center, Environmental and Occupational Health Sciences Institute, Rutgers University, Piscataway, New Jersey 08854, United States*; Email: Philip.demokritou@rutgers.edu

Authors

Hooman Parhizkar − *Department of Environmental and Occupational Health and Justice, School of Public Health, Rutgers University, Piscataway, New Jersey 08854, United States; Nanoscience and Advanced Materials Center, Environmental and Occupational Health Sciences Institute, Rutgers University, Piscataway, New Jersey 08854, United States*

Leonardo Calderon − *Nanoscience and Advanced Materials Center, Environmental and Occupational Health Sciences Institute, Rutgers University, Piscataway, New Jersey 08854, United States; School of Environmental and Biological Sciences, Department of Environmental Sciences, Rutgers, The State University of New Jersey, New Brunswick, New Jersey 08901, United States*

Denisa Lizonova − *Department of Environmental and Occupational Health and Justice, School of Public Health, Rutgers University, Piscataway, New Jersey 08854, United States; Nanoscience and Advanced Materials Center, Environmental and Occupational Health Sciences Institute, Rutgers University, Piscataway, New Jersey 08854, United States*

Irini Tsiodra − *Institute for Environmental Research and Sustainable Development, National Observatory of Athens, Athens 15236, Greece*

Nikolaos Mihalopoulos − *Institute for Environmental Research and Sustainable Development, National Observatory of Athens, Athens 15236, Greece; Environmental Chemical Processes Laboratory, Department of Chemistry, University of Crete, Heraklion 71003, Greece*

Ilias Kavouras − *Department of Environmental, Occupational and Geospatial Health Sciences, School of Public Health, City University of New York, New York, New York 10018, United States*

Mahbub Alam − *Center for Environmental Nanoscience and Risk, Department of Environmental Health Sciences, Arnold School of Public Health, University of South Carolina, Columbia, South Carolina 29208, United States*

Mohammed Baalousha − *Center for Environmental Nanoscience and Risk, Department of Environmental Health Sciences, Arnold School of Public Health, University of South Carolina, Columbia, South Carolina 29208, United States;* orcid.org/0000-0001-7491-4954

Lila Bazina − *Department of Environmental and Occupational Health and Justice, School of Public Health, Rutgers University, Piscataway, New Jersey 08854, United States; Nanoscience and Advanced Materials Center, Environmental and Occupational Health Sciences Institute, Rutgers University, Piscataway, New Jersey 08854, United States*

Georgios A. Kelesidis − *Department of Environmental and Occupational Health and Justice, School of Public Health, Rutgers University, Piscataway, New Jersey 08854, United States; Nanoscience and Advanced Materials Center, Environmental and Occupational Health Sciences Institute, Rutgers University, Piscataway, New Jersey 08854, United States*

Complete contact information is available at: https://pubs.acs.org/10.1021/acs.est.4c02016

Notes

The authors declare no competing financial interest.

ACKNOWLEDGMENTS

This investigation was made possible partly by funding from NIH grants num. 1R01HL168899-01A1 and 1R01HL168899. Its contents are solely the responsibility of the authors and do not necessarily represent the official views of the NIH. Additionally, research was supported by the Rutgers-NIEHS Center for Environmental Exposures and Disease (CEED) (NIH grant # P30ES005022). J.G.C.L. is supported by the Rutgers Presidential Faculty Fellowship and the Harvard JPB Environmental Fellowship Program.

REFERENCES

(1) Abatzoglou, J. T.; Williams, A. P. Impact of anthropogenic climate change on wildfire across western US forests. *Proc. Natl. Acad. Sci. U. S. A.* **2016**, *113* (42), 11770−11775. Xu, R.; Yu, P.; Abramson, M. J.; Johnston, F. H.; Samet, J. M.; Bell, M. L.; Haines, A.; Ebi, K. L.; Li, S.; Guo, Y. Wildfires, global climate change, and human health. *New England Journal of Medicine* **2020**, *383* (22), 2173−2181.

(2) Xie, Y.; Lin, M.; Decharme, B.; Delire, C.; Horowitz, L. W.; Lawrence, D. M.; Li, F.; Séférian, R. Tripling of western US particulate pollution from wildfires in a warming climate. *Proc. Natl. Acad. Sci. U.S.A.* **2022**, *119* (14), No. e2111372119. Ford, B.; Val Martin, M.; Zelasky, S.; Fischer, E.; Anenberg, S.; Heald, C. L.; Pierce, J. Future fire impacts on smoke concentrations, visibility, and health in the contiguous United States. *GeoHealth* **2018**, *2* (8), 229−247.

(3) Kreider, M. R.; Higuera, P. E.; Parks, S. A.; Rice, W. L.; White, N.; Larson, A. J. Fire suppression makes wildfires more severe and accentuates impacts of climate change and fuel accumulation. *Nat. Commun.* **2024**, *15* (1), 2412.

(4) NIFC, N. I. F. C.*Total Wildland Fires and Acres (1983−2022)*. National Interagency Fire Center, 2023. https://www.nifc.gov/fire-information/statistics/wildfires.

(5) Riley, K. L.; Loehman, R. A. Mid-21st-century climate changes increase predicted fire occurrence and fire season length, Northern Rocky Mountains, United States. *Ecosphere* **2016**, *7* (11), No. e01543, DOI: 10.1002/ecs2.1543.

(6) Huxley-Reicher, B.; Folger, M.; Casale, M. *Trouble in the Air: Millions of Americans breathed polluted air in 2020*; Environment California Research & Policy Center and CALPIRG Education Fund, 2021.

(7) EPA, U. S. *National Ambient Air Quality Standards (NAAQS) for Particulate Matter (PM)*. U.S. Environmental Protection Agency, 2024. https://www.epa.gov/pm-pollution/national-ambient-air-quality-standards-naaqs-pm#rule-summary.

(8) Xu, R.; Ye, T.; Yue, X.; Yang, Z.; Yu, W.; Zhang, Y.; Bell, M. L.; Morawska, L.; Yu, P.; Zhang, Y.; Wu, Y.; Liu, Y.; Johnston, F.; Lei, Y.; Abramson, M. J.; Guo, Y.; Li, S. Global population exposure to landscape fire air pollution from 2000 to 2019. *Nature* **2023**, *621* (7979), 521−529.
(9) Davies, I. P.; Haugo, R. D.; Robertson, J. C.; Levin, P. S. The unequal vulnerability of communities of color to wildfire. *PLoS One* **2018**, *13* (11), No. e0205825.
(10) Masri, S.; Jin, Y.; Wu, J. Compound Risk of Air Pollution and Heat Days and the Influence of Wildfire by SES across California, 2018−2020: Implications for Environmental Justice in the Context of Climate Change. *Climate* **2022**, *10* (10), 145.
(11) Burke, M.; Childs, M. L.; de la Cuesta, B.; Qiu, M.; Li, J.; Gould, C. F.; Heft-Neal, S.; Wara, M. The contribution of wildfire to PM2.5 trends in the USA. *Nature* **2023**, *622* (7984), 761−766.
(12) Makkonen, U.; Hellén, H.; Anttila, P.; Ferm, M. Size distribution and chemical composition of airborne particles in south-eastern Finland during different seasons and wildfire episodes in 2006. *Sci. Total Environ.* **2010**, *408* (3), 644−651.
(13) Verma, V.; Polidori, A.; Schauer, J. J.; Shafer, M. M.; Cassee, F. R.; Sioutas, C. Physicochemical and Toxicological Profiles of Particulate Matter in Los Angeles during the October 2007 Southern California Wildfires. *Environ. Sci. Technol.* **2009**, *43* (3), 954−960.
(14) Boaggio, K.; LeDuc, S. D.; Rice, R. B.; Duffney, P. F.; Foley, K. M.; Holder, A. L.; McDow, S.; Weaver, C. P. Beyond particulate matter mass: heightened levels of lead and other pollutants associated with destructive fire events in California. *Environ. Sci. Technol.* **2022**, *56* (20), 14272−14283.
(15) Dong, T. T. T.; Hinwood, A. L.; Callan, A. C.; Zosky, G.; Stock, W. D. In vitro assessment of the toxicity of bushfire emissions: A review. *Sci. Total Environ.* **2017**, *603-604*, 268−278.
(16) Chakrabarty, R. K.; Shetty, N. J.; Thind, A. S.; Beeler, P.; Sumlin, B. J.; Zhang, C.; Liu, P.; Idrobo, J. C.; Adachi, K.; Wagner, N. L.; Schwarz, J. P.; Ahern, A.; Sedlacek, A. J.; Lambe, A.; Daube, C.; Lyu, M.; Liu, C.; Herndon, S.; Onasch, T. B.; Mishra, R. Shortwave absorption by wildfire smoke dominated by dark brown carbon. *Nature Geoscience* **2023**, *16* (8), 683−688.
(17) Gyawali, M.; Arnott, W. P.; Lewis, K.; Moosmüller, H. In situ aerosol optics in Reno, NV, USA during and after the summer 2008 California wildfires and the influence of absorbing and non-absorbing organic coatings on spectral light absorption. *Atmos. Chem. Phys.* **2009**, *9* (20), 8007−8015.
(18) Kim, Y. H.; Warren, S. H.; Krantz, Q. T.; King, C.; Jaskot, R.; Preston, W. T.; George, B. J.; Hays, M. D.; Landis, M. S.; Higuchi, M.; DeMarini, D. M.; Gilmour, M. I. Mutagenicity and Lung Toxicity of Smoldering vs. Flaming Emissions from Various Biomass Fuels: Implications for Health Effects from Wildland Fires. *Environ. Health Perspect.* **2018**, *126* (1), No. 017011.
(19) Singh, D.; Tassew, D. D.; Nelson, J.; Chalbot, M.-C. G.; Kavouras, I. G.; Tesfaigzi, Y.; Demokritou, P. Physicochemical and toxicological properties of wood smoke particulate matter as a function of wood species and combustion condition. *Journal of Hazardous Materials* **2023**, *441*, No. 129874.
(20) Singh, D.; Tassew, D. D.; Nelson, J.; Chalbot, M.-C. G.; Kavouras, I. G.; Demokritou, P.; Tesfaigzi, Y. Development of an Integrated Platform to Assess the Physicochemical and Toxicological Properties of Wood Combustion Particulate Matter. *Chem. Res. Toxicol.* **2022**, *35* (9), 1541−1557.
(21) Schlosser, J. S.; Braun, R. A.; Bradley, T.; Dadashazar, H.; MacDonald, A. B.; Aldhaif, A. A.; Aghdam, M. A.; Mardi, A. H.; Xian, P.; Sorooshian, A. Analysis of aerosol composition data for western United States wildfires between 2005 and 2015: Dust emissions, chloride depletion, and most enhanced aerosol constituents. *Journal of Geophysical Research: Atmospheres* **2017**, *122* (16), 8951−8966. Sparks, T. L.; Wagner, J. Composition of particulate matter during a wildfire smoke episode in an urban area. *Aerosol Sci. Technol.* **2021**, *55* (6), 734−747.
(22) Holder, A. L.; Ahmed, A.; Vukovich, J. M.; Rao, V.; Amon, C. H. Hazardous air pollutant emissions estimates from wildfires in the wildland urban interface. *PNAS Nexus* **2023**, *2* (6), pgad186 DOI: 10.1093/pnasnexus/pgad186.
(23) Aguilera, R.; Corringham, T.; Gershunov, A.; Benmarhnia, T. Wildfire smoke impacts respiratory health more than fine particles from other sources: observational evidence from Southern California. *Nat. Commun.* **2021**, *12* (1), 1493.
(24) Cascio, W. E. Wildland fire smoke and human health. *Science of the total environment* **2018**, *624*, 586−595.
(25) Liu, J. C.; Wilson, A.; Mickley, L. J.; Dominici, F.; Ebisu, K.; Wang, Y.; Sulprizio, M. P.; Peng, R. D.; Yue, X.; Son, J.-Y. Wildfire-specific fine particulate matter and risk of hospital admissions in urban and rural counties. *Epidemiology* **2017**, *28* (1), 77. McArdle, C. E.; Dowling, T. C.; Carey, K.; DeVies, J.; Johns, D.; Gates, A. L.; Stein, Z.; van Santen, K. L.; Radhakrishnan, L.; Kite-Powell, A.; Soetebier, K.; Sacks, J. D.; Sircar, K.; Hartnett, K. P.; Mirabelli, M. C. Asthma-Associated Emergency Department Visits During the Canadian Wildfire Smoke Episodes—United States, April−August 2023. *Morb. Mortal. Wkly. Rep.* **2023**, *72*, 926.
(26) Ye, T.; Guo, Y.; Chen, G.; Yue, X.; Xu, R.; Coêlho, M. d. S. Z. S.; Saldiva, P. H. N.; Zhao, Q.; Li, S. Risk and burden of hospital admissions associated with wildfire-related PM2· 5 in Brazil, 2000−15: a nationwide time-series study. *Lancet Planetary Health* **2021**, *5* (9), e599−e607.
(27) Chen, H.; Samet, J. M.; Bromberg, P. A.; Tong, H. Cardiovascular health impacts of wildfire smoke exposure. *Part. Fibre Toxicol.* **2021**, *18*, 1−22. Jones, C. G.; Rappold, A. G.; Vargo, J.; Cascio, W. E.; Kharrazi, M.; McNally, B.; Hoshiko, S.; CARES Surveillance Group. Out-of-hospital cardiac arrests and wildfire-related particulate matter during 2015−2017 California wildfires. *J. Am. Heart Assoc.* **2020**, *9* (8), No. e014125.
(28) Zhang, B.; Weuve, J.; Langa, K. M.; D'Souza, J.; Szpiro, A.; Faul, J.; Mendes de Leon, C.; Gao, J.; Kaufman, J. D.; Sheppard, L.; Lee, J.; Kobayashi, L. C.; Hirth, R.; Adar, S. D. Comparison of Particulate Air Pollution From Different Emission Sources and Incident Dementia in the US. *JAMA Internal Medicine* **2023**, *183* (10), 1080−1089.
(29) Chen, G.; Guo, Y.; Yue, X.; Tong, S.; Gasparrini, A.; Bell, M. L.; Armstrong, B.; Schwartz, J.; Jaakkola, J. J. K.; Zanobetti, A.; Lavigne, E.; Saldiva, P. H. N.; Kan, H.; Royé, D.; Milojevic, A.; Overcenco, A.; Urban, A.; Schneider, A.; Entezari, A.; Vicedo-Cabrera, A. M.; Zeka, A.; Tobias, A.; Nunes, B.; Alahmad, B.; Forsberg, B.; Pan, S. C.; Íñiguez, C.; Ameling, C.; De la Cruz Valencia, C.; Åström, C.; Houthuijs, D.; Van Dung, D.; Samoli, E.; Mayvaneh, F.; Sera, F.; Carrasco-Escobar, G.; Lei, Y.; Orru, H.; Kim, H.; Holobaca, I. H.; Kyselý, J.; Teixeira, J. P.; Madureira, J.; Katsouyanni, K.; Hurtado-Díaz, M.; Maasikmets, M.; Ragettli, M. S.; Hashizume, M.; Stafoggia, M.; Pascal, M.; Scortichini, M.; de Sousa Zanotti Stagliorio Coêlho, M.; Ortega, N. V.; Ryti, N. R. I.; Scovronick, N.; Matus, P.; Goodman, P.; Garland, R. M.; Abrutzky, R.; Garcia, S. O.; Rao, S.; Fratianni, S.; Dang, T. N.; Colistro, V.; Huber, V.; Lee, W.; Seposo, X.; Honda, Y.; Guo, Y. L.; Ye, T.; Yu, W.; Abramson, M. J.; Samet, J. M.; Li, S. Mortality risk attributable to wildfire-related PM2· 5 pollution: a global time series study in 749 locations. *Lancet Planet. Health* **2021**, *5* (9), e579−e587.
(30) NRCan. *Canada's Record-Breaking Wildfires 2023: A Fiery Wake-up Call*. Government of Canada, 2023. https://natural-resources.canada.ca/simply-science/canadas-record-breaking-wildfires-2023-fiery-wake-call/25303.
(31) Voiland, A. *Smoke Smothers the Northeast*. NASA Earth Observatory, 2023. https://earthobservatory.nasa.gov/images/151433/smoke-smothers-the-northeast.
(32) Chen, L. W. A.; Chow, J. C.; Doddridge, B. G.; Dickerson, R. R.; Ryan, W. F.; Mueller, P. K. Analysis of a Summertime PM2.5 and Haze Episode in the Mid-Atlantic Region. *J. Air Waste Manage. Assoc.* **2003**, *53* (8), 946−956.
(33) Demokritou, P.; Lee, S. J.; Ferguson, S. T.; Koutrakis, P. A compact multistage (cascade) impactor for the characterization of atmospheric aerosols. *J. Aerosol Sci.* **2004**, *35* (3), 281−299.
(34) Sotiriou, G. A.; Singh, D.; Zhang, F.; Wohlleben, W.; Chalbot, M.-C. G.; Kavouras, I. G.; Demokritou, P. An integrated methodology for the assessment of environmental health implications during thermal

decomposition of nano-enabled products. *Environmental Science: Nano* **2015**, *2* (3), 262−272.
(35) Tsiodra, I.; Grivas, G.; Tavernaraki, K.; Bougiatioti, A.; Apostolaki, M.; Paraskevopoulou, D.; Gogou, A.; Parinos, C.; Oikonomou, K.; Tsagkaraki, M.; Zarmpas, P.; Nenes, A.; Mihalopoulos, N. Annual exposure to polycyclic aromatic hydrocarbons in urban environments linked to wintertime wood-burning episodes. *Atmospheric Chemistry and Physics* **2021**, *21* (23), 17865−17883.
(36) Cavalli, F.; Viana, M.; Yttri, K. E.; Genberg, J.; Putaud, J.-P. Toward a standardised thermal-optical protocol for measuring atmospheric organic and elemental carbon: the EUSAAR protocol. *Atmos. Meas. Tech. Discuss.* **2009**, *2* (5), 2321−2345.
(37) Alam, M.; Alshehri, T.; Wang, J.; Singerling, S. A.; Alpers, C. N.; Baalousha, M. Identification and quantification of Cr, Cu, and As incidental nanomaterials derived from CCA-treated wood in wildland-urban interface fire ashes. *Journal of Hazardous Materials* **2023**, *445*, No. 130608. Baalousha, M.; Wang, J.; Erfani, M.; Goharian, E. Elemental fingerprints in natural nanomaterials determined using SP-ICP-TOF-MS and clustering analysis. *Science of The Total Environment* **2021**, *792*, No. 148426. Wang, J.; Nabi, M. M.; Erfani, M.; Goharian, E.; Baalousha, M. Identification and quantification of anthropogenic nanomaterials in urban rain and runoff using single particle-inductively coupled plasma-time of flight-mass spectrometry. *Environmental Science: Nano* **2022**, *9* (2), 714−729.
(38) Anjilvel, S.; Asgharian, B. A Multiple-Path Model of Particle Deposition in the Rat Lung. *Fundam. Appl. Toxicol.* **1995**, *28* (1), 41−50. Price, O. T.; Asgharian, B.; Miller, F. J.; Cassee, F. R.; de Winter-Sorkina, R. Multiple Path Particle Dosimetry model (MPPD v1. 0): A model for human and rat airway particle dosimetry. *RIVM rapport 650010030* **2002**. Asgharian, B.; Hofmann, W.; Bergmann, R. Particle deposition in a multiple-path model of the human lung. *Aerosol Science & Technology* **2001**, *34* (4), 332−339. Asgharian, B.; Price, O.; Oldham, M.; Chen, L.-C.; Saunders, E.; Gordon, T.; Mikheev, V. B.; Minard, K. R.; Teeguarden, J. G. Computational modeling of nanoscale and microscale particle deposition, retention and dosimetry in the mouse respiratory tract. *Inhalation toxicology* **2014**, *26* (14), 829−842.
(39) Yeh, H.-C.; Schum, G. Models of human lung airways and their application to inhaled particle deposition. *Bull. Math. Biol.* **1980**, *42* (3), 461−480.
(40) Martin, J.; Bello, D.; Bunker, K.; Shafer, M.; Christiani, D.; Woskie, S.; Demokritou, P. Occupational exposure to nanoparticles at commercial photocopy centers. *Journal of Hazardous Materials* **2015**, *298*, 351−360.
(41) Bein, K. J.; Zhao, Y.; Johnston, M. V.; Wexler, A. S. Interactions between boreal wildfire and urban emissions. *J. Geophys. Res.: Atmos.* **2008**, *113* (D7), D07304 DOI: 10.1029/2007JD008910.
(42) Park, S. S.; Harrison, D.; Pancras, J. P.; Ondov, J. M. Highly time-resolved organic and elemental carbon measurements at the Baltimore Supersite in 2002. *J. Geophys. Res.: Atmos.* **2005**, *110* (D7), D07S06 DOI: 10.1029/2004JD004610.
(43) Zu, K.; Tao, G.; Long, C.; Goodman, J.; Valberg, P. Long-range fine particulate matter from the 2002 Quebec forest fires and daily mortality in Greater Boston and New York City. *Air Quality, Atmosphere & Health* **2016**, *9* (3), 213−221. Sapkota, A.; Symons, J. M.; Kleissl, J.; Wang, L.; Parlange, M. B.; Ondov, J.; Breysse, P. N.; Diette, G. B.; Eggleston, P. A.; Buckley, T. J. Impact of the 2002 Canadian forest fires on particulate matter air quality in Baltimore City. *Environ. Sci. Technol.* **2005**, *39* (1), 24−32.
(44) Kelesidis, G. A.; Bruun, C. A.; Pratsinis, S. E. The impact of organic carbon on soot light absorption. *Carbon* **2021**, *172*, 742−749.
(45) Zhu, Y.; Hinds, W. C.; Kim, S.; Sioutas, C. Concentration and Size Distribution of Ultrafine Particles Near a Major Highway. *J. Air Waste Manage. Assoc.* **2002**, *52* (9), 1032−1042.
(46) Chomanee, J.; Thongboon, K.; Tekasakul, S.; Furuuchi, M.; Dejchanchaiwong, R.; Tekasakul, P. Physicochemical and toxicological characteristics of nanoparticles in aerosols in southern Thailand during recent haze episodes in lower southeast Asia. *Journal of Environmental Sciences* **2020**, *94*, 72−80. Mahasakpan, N.; Chaisongkaew, P.; Inerb, M.; Nim, N.; Phairuang, W.; Tekasakul, S.; Furuuchi, M.; Hata, M.; Kaosol, T.; Tekasakul, P.; Dejchanchaiwong, R. Fine and ultrafine particle- and gas-polycyclic aromatic hydrocarbons affecting southern Thailand air quality during transboundary haze and potential health effects. *J. Environ. Sci.* **2023**, *124*, 253−267.
(47) Hong, L.; Liu, G.; Zhou, L.; Li, J.; Xu, H.; Wu, D. Emission of organic carbon, elemental carbon and water-soluble ions from crop straw burning under flaming and smoldering conditions. *Particuology* **2017**, *31*, 181−190.
(48) Saleh, R.; Hennigan, C. J.; McMeeking, G. R.; Chuang, W. K.; Robinson, E. S.; Coe, H.; Donahue, N. M.; Robinson, A. L. Absorptivity of brown carbon in fresh and photo-chemically aged biomass-burning emissions. *Atmos. Chem. Phys.* **2013**, *13* (15), 7683−7693.
(49) Carter, T. S.; Heald, C. L.; Cappa, C. D.; Kroll, J. H.; Campos, T. L.; Coe, H.; Cotterell, M. I.; Davies, N. W.; Farmer, D. K.; Fox, C.; Garofalo, L. A.; Hu, L.; Langridge, J. M.; Levin, E. J. T.; Murphy, S. M.; Pokhrel, R. P.; Shen, Y.; Szpek, K.; Taylor, J. W.; Wu, H. Investigating Carbonaceous Aerosol and Its Absorption Properties From Fires in the Western United States (WE-CAN) and Southern Africa (ORACLES and CLARIFY). *Journal of Geophysical Research: Atmospheres* **2021**, *126* (15), No. e2021JD034984. Holder, A. L.; Hagler, G. S. W.; Aurell, J.; Hays, M. D.; Gullett, B. K. Particulate matter and black carbon optical properties and emission factors from prescribed fires in the south-eastern United States. *Journal of Geophysical Research: Atmospheres* **2016**, *121* (7), 3465−3483. May, A. A.; McMeeking, G. R.; Lee, T.; Taylor, J. W.; Craven, J. S.; Burling, I.; Sullivan, A. P.; Akagi, S.; Collett, J. L., Jr.; Flynn, M.; Coe, H.; Urbanski, S. P.; Seinfeld, J. H.; Yokelson, R. J.; Kreidenweis, S. M. Aerosol emissions from prescribed fires in the United States: A synthesis of laboratory and aircraft measurements. *J. Geophys. Res.: Atmos.* **2014**, *119* (20), 11826−811849. Selimovic, V.; Yokelson, R. J.; McMeeking, G. R.; Coefield, S. In situ measurements of trace gases, PM, and aerosol optical properties during the 2017 NW US wildfire smoke event. *Atmos. Chem. Phys.* **2019**, *19* (6), 3905−3926. Wang, X.; Heald, C. L.; Sedlacek, A. J.; de Sá, S. S.; Martin, S. T.; Alexander, M. L.; Watson, T. B.; Aiken, A. C.; Springston, S. R.; Artaxo, P. Deriving brown carbon from multiwavelength absorption measurements: method and application to AERONET and Aethalometer observations. *Atmos. Chem. Phys.* **2016**, *16* (19), 12733−12752. Lack, D. A.; Langridge, J. M.; Bahreini, R.; Cappa, C. D.; Middlebrook, A. M.; Schwarz, J. P. Brown carbon and internal mixing in biomass burning particles. *Proc. Natl. Acad. Sci. U. S. A.* **2012**, *109* (37), 14802−14807.
(50) Wentworth, G. R.; Aklilu, Y.-a.; Landis, M. S.; Hsu, Y.-M. Impacts of a large boreal wildfire on ground level atmospheric concentrations of PAHs, VOCs and ozone. *Atmos. Environ.* **2018**, *178*, 19−30. Kohl, L.; Meng, M.; de Vera, J.; Bergquist, B.; Cooke, C. A.; Hustins, S.; Jackson, B.; Chow, C. W.; Chan, A. W. Limited retention of wildfire-derived PAHs and trace elements in indoor environments. *Geophys. Res. Lett.* **2019**, *46* (1), 383−391.
(51) Vicente, A.; Alves, C.; Monteiro, C.; Nunes, T.; Mirante, F.; Cerqueira, M.; Calvo, A.; Pio, C. Organic speciation of aerosols from wildfires in central Portugal during summer 2009. *Atmos. Environ.* **2012**, *57*, 186−196.
(52) De La Torre-Roche, R. J.; Lee, W.-Y.; Campos-Díaz, S. I. Soil-borne polycyclic aromatic hydrocarbons in El Paso, Texas: Analysis of a potential problem in the United States/Mexico border region. *Journal of Hazardous Materials* **2009**, *163* (2), 946−958. Tobiszewski, M.; Namieśnik, J. PAH diagnostic ratios for the identification of pollution emission sources. *Environ. Pollut.* **2012**, *162*, 110−119.
(53) Dvorská, A.; Lammel, G.; Klánová, J.; et al. *Atmos. Environ.* **2011**, *45* (2), 420−427.
(54) Nelson, J.; Chalbot, M.-C. G.; Tsiodra, I.; Mihalopoulos, N.; Kavouras, I. G. Physicochemical characterization of personal exposures to smoke aerosol and PAHs of wildland firefighters in prescribed fires. *Exposure and Health* **2021**, *13*, 105−118.
(55) Zhang, Y.; Yang, L.; Gao, Y.; Chen, J.; Li, Y.; Jiang, P.; Zhang, J.; Yu, H.; Wang, W. Comparative Study of PAHs in PM1 and PM2.5 at a Background Site in the North China Plain. *Aerosol and Air Quality Research* **2019**, *19* (10), 2281−2293.

(56) Wu, S.-P.; Qian, R.-R.; Lee, T.-C.; Wang, X.-H.; Hong, H.-S.; Yuan, C.-S. Seasonal variation for the ratio of BaP to BeP at different sites in Great Xiamen Bay. *J. Environ. Monit.* **2012**, *14* (4), 1221−1229.
(57) Alshehri, T.; Wang, J.; Singerling, S. A.; Gigault, J.; Webster, J. P.; Matiasek, S. J.; Alpers, C. N.; Baalousha, M. Wildland-urban interface fire ashes as a major source of incidental nanomaterials. *Journal of Hazardous Materials* **2023**, *443*, No. 130311. Isley, C. F.; Taylor, M. P. Atmospheric remobilization of natural and anthropogenic contaminants during wildfires. *Environ. Pollut.* **2020**, *267*, No. 115400.
(58) Verma, V.; Shafer, M. M.; Schauer, J. J.; Sioutas, C. Contribution of transition metals in the reactive oxygen species activity of PM emissions from retrofitted heavy-duty vehicles. *Atmos. Environ.* **2010**, *44* (39), 5165−5173. Tacu, I.; Kokalari, I.; Abollino, O.; Albrecht, C.; Malandrino, M.; Ferretti, A. M.; Schins, R. P. F.; Fenoglio, I. Mechanistic Insights into the Role of Iron, Copper, and Carbonaceous Component on the Oxidative Potential of Ultrafine Particulate Matter. *Chem. Res. Toxicol.* **2021**, *34* (3), 767−779. Bates, J. T.; Fang, T.; Verma, V.; Zeng, L.; Weber, R. J.; Tolbert, P. E.; Abrams, J. Y.; Sarnat, S. E.; Klein, M.; Mulholland, J. A.; Russell, A. G. Review of Acellular Assays of Ambient Particulate Matter Oxidative Potential: Methods and Relationships with Composition, Sources, and Health Effects. *Environ. Sci. Technol.* **2019**, *53* (8), 4003−4019.
(59) Lopez, A. M.; Pacheco, J. L.; Fendorf, S. Metal toxin threat in wildland fires determined by geology and fire severity. *Nat. Commun.* **2023**, *14* (1), 8007.
(60) Mylonaki, M.; Gini, M.; Georgopoulou, M.; Pilou, M.; Chalvatzaki, E.; Solomos, S.; Diapouli, E.; Giannakaki, E.; Lazaridis, M.; Pandis, S. N.; Nenes, A.; Eleftheriadis, K.; Papayannis, A. Wildfire and African dust aerosol oxidative potential, exposure and dose in the human respiratory tract. *Science of The Total Environment* **2024**, *913*, No. 169683. Miller, F. J.; Asgharian, B.; Schroeter, J. D.; Price, O. Improvements and additions to the Multiple Path Particle Dosimetry model. *J. Aerosol Sci.* **2016**, *99*, 14−26. Asgharian, B.; Anjilvel, S. A Multiple-Path Model of Fiber Deposition in the Rat Lung. *Toxicol. Sci.* **1998**, *44* (1), 80−86.
(61) Jariyasopit, N.; Tung, P.; Su, K.; Halappanavar, S.; Evans, G. J.; Su, Y.; Khoomrung, S.; Harner, T. Polycyclic aromatic compounds in urban air and associated inhalation cancer risks: A case study targeting distinct source sectors. *Environmental pollution* **2019**, *252*, 1882−1891. Ranjbar, M.; Rotondi, M. A.; Ardern, C. I.; Kuk, J. L. Urinary biomarkers of polycyclic aromatic hydrocarbons are associated with cardiometabolic health risk. *PloS one* **2015**, *10* (9), No. e0137536. Armstrong, B.; Hutchinson, E.; Unwin, J.; Fletcher, T. Lung cancer risk after exposure to polycyclic aromatic hydrocarbons: a review and meta-analysis. *Environ. Health Perspect.* **2004**, *112* (9), 970−978.
(62) Meek, H. C. Notes from the Field: Asthma-Associated Emergency Department Visits During a Wildfire Smoke Event—New York, June 2023. *Morb. Mortal. Wkly. Rep.* **2023**, *72*, 933.
(63) Thurston, G.; Yu, W.; Luglio, D. An Evaluation of the Asthma Impact of the June 2023 New York City Wildfire Air Pollution Episode. *American Journal of Respiratory and Critical Care Medicine* **2023**, *208* (8), 898−900.
(64) Flood-Garibay, J. A.; Angulo-Molina, A.; Méndez-Rojas, M. Á. Particulate matter and ultrafine particles in urban air pollution and their effect on the nervous system. *Environmental Science: Processes & Impacts* **2023**, *25* (4), 704−726. Slezakova, K.; Morais, S.; do Carmo Pereira, M. Atmospheric nanoparticles and their impacts on public health. In *Curr. Top. Public Health*; IntechOpen, 2013 DOI: 10.5772/54775. González-Maciel, A.; Reynoso-Robles, R.; Torres-Jardon, R.; Mukherjee, P. S.; Calderón-Garcidueñas, L. Combustion-derived nanoparticles in key brain target cells and organelles in young urbanites: culprit hidden in plain sight in Alzheimer's disease development. *J. Alzheimer's Dis.* **2017**, *59* (1), 189−208.
(65) Wettstein, Z. S.; Hoshiko, S.; Fahimi, J.; Harrison, R. J.; Cascio, W. E.; Rappold, A. G. Cardiovascular and Cerebrovascular Emergency Department Visits Associated With Wildfire Smoke Exposure in California in 2015. *Journal of the American Heart Association* **2018**, *7* (8), No. e007492.
(66) To, P.; Eboreime, E.; Agyapong, V. I. O. The Impact of Wildfires on Mental Health: A Scoping Review. *Behavioral Sciences* **2021**, *11* (9), 126.
(67) Wen, J.; Burke, M. Lower test scores from wildfire smoke exposure. *Nature Sustainability* **2022**, *5* (11), 947−955.
(68) Heft-Neal, S.; Driscoll, A.; Yang, W.; Shaw, G.; Burke, M. Associations between wildfire smoke exposure during pregnancy and risk of preterm birth in California. *Environmental Research* **2022**, *203*, No. 111872.
(69) Park, B. Y.; Boles, I.; Monavvari, S.; Patel, S.; Alvarez, A.; Phan, M.; Perez, M.; Yao, R. The association between wildfire exposure in pregnancy and foetal gastroschisis: A population-based cohort study. *Paediatric and Perinatal Epidemiology* **2022**, *36* (1), 45−53.
(70) Padula, A. M.; Noth, E. M.; Hammond, S. K.; Lurmann, F. W.; Yang, W.; Tager, I. B.; Shaw, G. M. Exposure to airborne polycyclic aromatic hydrocarbons during pregnancy and risk of preterm birth. *Environmental Research* **2014**, *135*, 221−226.
(71) Ramdahl, T. Retene—a molecular marker of wood combustion in ambient air. *Nature* **1983**, *306* (5943), 580−582.
(72) Alves, C. A.; Vicente, A. M.; Custódio, D.; Cerqueira, M.; Nunes, T.; Pio, C.; Lucarelli, F.; Calzolai, G.; Nava, S.; Diapouli, E.; Eleftheriadis, K.; Querol, X.; Bandowe, B. A. M. Polycyclic aromatic hydrocarbons and their derivatives (nitro-PAHs, oxygenated PAHs, and azaarenes) in PM2. 5 from Southern European cities. *Sci. Total Environ.* **2017**, *595*, 494−504.
(73) Peixoto, M. S.; da Silva Junior, F. C.; de Oliveira Galvão, M. F.; Roubicek, D. A.; de Oliveira Alves, N.; Batistuzzo de Medeiros, S. R. Oxidative stress, mutagenic effects, and cell death induced by retene. *Chemosphere* **2019**, *231*, 518−527.
(74) Scaramboni, C.; Arruda Moura Campos, M. L.; Junqueira Dorta, D.; Palma de Oliveira, D.; Batistuzzo de Medeiros, S. R.; de Oliveira Galvão, M. F.; Dreij, K. Reactive oxygen species-dependent transient induction of genotoxicity by retene in human liver HepG2 cells. *Toxicology in Vitro* **2023**, *91*, No. 105628.
(75) Sarma, S. N.; Blais, J. M.; Chan, H. M. Neurotoxicity of alkylated polycyclic aromatic compounds in human neuroblastoma cells. *Journal of Toxicology and Environmental Health, Part A* **2017**, *80* (5), 285−300.
(76) Hawliczek, A.; Nota, B.; Cenijn, P.; Kamstra, J.; Pieterse, B.; Winter, R.; Winkens, K.; Hollert, H.; Segner, H.; Legler, J. Developmental toxicity and endocrine disrupting potency of 4-azapyrene, benzo[b]fluorene and retene in the zebrafish Danio rerio. *Reproductive Toxicology* **2012**, *33* (2), 213−223.
(77) Samburova, V.; Zielinska, B.; Khlystov, A. Do 16 Polycyclic Aromatic Hydrocarbons Represent PAH Air Toxicity? *Toxics* **2017**, *5* (3), 17.
(78) Gould, C. F.; Heft-Neal, S.; Johnson, M.; Aguilera, J.; Burke, M.; Nadeau, K. Health Effects of Wildfire Smoke Exposure. *Annu. Rev. Med.* **2024**, *75*, 277−292. Black, C.; Tesfaigzi, Y.; Bassein, J. A.; Miller, L. A. Wildfire smoke exposure and human health: Significant gaps in research for a growing public health issue. *Environmental Toxicology and Pharmacology* **2017**, *55*, 186−195.

https://doi.org/10.1021/acs.est.4c02016
Environ. Sci. Technol. XXXX, XXX, XXX−XXX